

## Forced and Rotary Convection around a Cone of Revolution

Christine LETICIA<sup>1\*</sup>, Ulrich CANISSIUS<sup>2</sup> and Edouard ALIDINA<sup>1</sup>

<sup>1</sup>Laboratoire de Mécanique des Fluides et Systèmes Energétiques Appliqués (MFSEA), Faculté des Sciences, Université d'Antsirana, B.P.O, Antsirana 201, Madagascar

<sup>2</sup>Laboratoire de Mécanique et de Métrologie, Ecole Normale Supérieure pour l'Enseignement Technique, Université d'Antsirana, Antsirana 201, Madagascar

**ABSTRACT:** A numerical study of transfers by forced laminar convection around a cone rotating around an inclined axis of revolution is presented. The flow, of the boundary layer type, is ascending vertical and the fluid considered is Newtonian. The speed outside the boundary layer is determined by [7]. Using a numerical model, the continuity, Navier-Stokes and energy conservation equations are solved by an implicit finite difference method. The influence of the rotation parameter  $B$  on transfers is analyzed. The results are presented by the temperatures profiles, the meridian velocity, the normal velocity, the Nusselt number and as well as the meridian friction coefficient.

**KEYWORDS:** three-dimensional forced and rotary convection, three-dimensional boundary layer, cone of revolution, heat transfer, numerical study.

Date of Submission: 28-10-2020

Date of acceptance: 09-11-2020

### Nomenclature

#### Roman letter

$a$	thermal diffusivity of fluid, ( $m^2.s^{-1}$ )
$Cf_u$	meridian friction coefficient
$Cf_w$	azimuthal friction coefficient
$C_p$	specific heat capacity at constant pressure of the fluid, ( $J.kg^{-1}.K^{-1}$ )
$C_{for}$	predominance coefficient of forced convection
$C_{rot}$	predominance coefficient of rotatory convection
$L$	length generative, (m)
$N_u$	local Nusselt number
$Ec$	Ekert number
$Pr$	Prandtl number
$r$	normal distance from the projected M of a point P of the fluid to the axis of revolution of revolution of the cone, (m)
$Re_\infty$	Reynold number
$Re_\omega$	rotation Reynold number
$B$	rotation parameter
$T$	temperature of the fluid, (K)
$T_p$	temperature of the wall, (K)
$T_\infty$	temperature of the fluid away from the wall, (K)
$U_e$	modulus of external speed
$U_{e_x}, U_{e_\phi}$	components meridian and azimuthal of external speed, ( $m.s^{-1}$ )
$U_\infty$	flow velocity upstream of the body [ $m.s^{-1}$ ]
$V_x, V_y, V_\phi$	velocity component in x, y, and $\phi$ , ( $m.s^{-1}$ )
$x, y$	meridian and normal coordinates, (m)

#### Greek letter

$\phi$	azimuthal coordinate, (o)
$\lambda$	thermal conductivity, ( $W.m^{-1}.K^{-1}$ )

$\omega$	speed angular rotation of the cone (rad. s <sup>-2</sup> )
$\alpha$	angle of inclination, (°)
$\nu$	kinematic viscosity, (m <sup>2</sup> s <sup>-1</sup> )
$\theta_0$	demi-angle of opening of cone,(°)

### Indices / exponents

+ dimensionless variables

## I. INTRODUCTION

Although many theoretical and experimental studies have been carried out on convective transfers in the vicinity of a cone of revolution, most of the work only concerns natural or forced convection around a rotating vertical cone [2] or immobile and inclined [7]. The latter studied three-dimensional convective transfers around a cone of revolution closed on its upper part by a spherical cap and inclined with respect to the vertical. He determined the distribution of the velocity outside the boundary layer using the singularity method, and analyzed the influence of the angle of inclination of the cone and the heat transfer in the boundary layer that develops around this cone. Abdallah *et al.* [4] dedicated a numerical study of natural convection around an inclined cone of revolution. Thus, they studied the influence of the inclination angle of the cone on heat transfer. For this work, the objective is to analyze by a numerical simulation, the influence of the speed of rotation on the thermal and dynamic behavior of a laminar flow in forced and rotatory convection around its axis of revolution.

## II. THEORETICAL FOUNDATIONS

The physical model considered consists of a vertical cone of revolution, rotating around its axis of revolution and immersed in a forced flow of a Newtonian fluid with an ascending vertical direction (Figure 1).

### 2.1. Simplifying assumptions

In addition to these considerations and the classic boundary layer assumptions, we make the following additional assumptions:

- the cone rotating around the axis of revolution,
- transfers are three-dimensional, laminar and permanent,
- transfers by radiation and dissipation of viscous energy are negligible,
- the fluid is air, the physical properties of which are assumed to be constant.

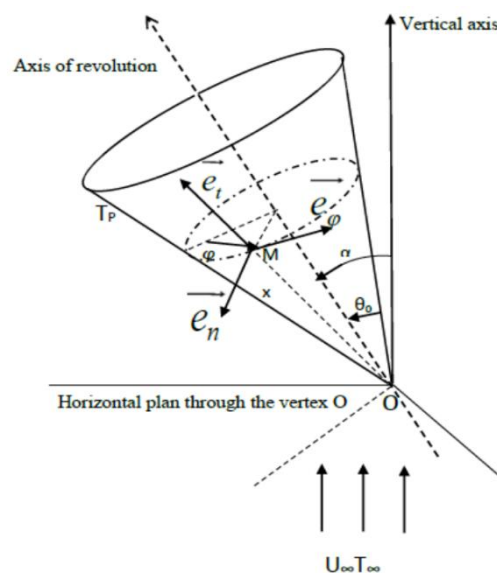


Figure 1. physical model and co-ordinates system

**2.2. Conservation equations in the boundary layer**

The reference sizes

$$x_+ = \frac{x}{L} y_+ = \frac{y}{L} \sqrt{Re_\infty} C_1 \varphi_+ = \varphi r_+ = \frac{r}{L}$$

$$V_x^+ = \frac{V_x}{U_\infty} C_2 V_y^+ = \frac{V_y}{U_\infty} \sqrt{Re_\infty} C_3 V_\varphi^+ = \frac{V_\varphi}{U_\infty} C_2 Ue^+ = \frac{Ue}{U_\infty} C_4$$

$$Ue_x^+ = \frac{Ue_x}{U_\infty} Ue_\varphi^+ = \frac{Ue_\varphi}{U_\infty} T^+ = \frac{(T - T_\infty)}{\frac{1}{2} \frac{U_\infty^2}{c_p}} C_5$$

With:

$$C_1 = \frac{Cfor + B^{\frac{1}{2}}Crot}{Cfor + Crot} C_3 = \frac{Cfor + B^{-\frac{1}{2}}Crot}{Cfor + Crot} C_5 = \frac{Cfor + B^{-2}Crot}{Cfor + Crot}$$

$$C_2 = \frac{Cfor + B^{-1}Crot}{Cfor + Crot} C_4 = \frac{Cfor + B^{-1}Re_\omega^{\frac{1}{2}}Crot}{Cfor + Crot}$$

$B = \frac{Re_\omega}{Re_\infty}$  : Rotation parameter

$Re_\omega = \frac{\omega L^2}{\nu}$  : Rotating Reynold number

Moreover, in order to highlight the individual or simultaneous contributions of a predominance, it is possible to associate respectively with each of these convections the points Cfor and Crot according to the type of the corresponding convection.

• **Equation of continuity**

$$\frac{\partial V_x^+}{\partial x_+} + \frac{C_1 C_2}{C_3} \frac{\partial V_y^+}{\partial y_+} + \frac{V_x^+}{r^+} \frac{dr^+}{dx_+} + \frac{1}{r^+} \frac{\partial V_\varphi^+}{\partial \varphi_+} = 0 \quad (1)$$

• **Momentum equations**

$$V_x^+ \frac{\partial V_x^+}{\partial x_+} + \frac{C_1 C_2}{C_3} V_y^+ \frac{\partial V_x^+}{\partial y_+} + \frac{V_\varphi^+}{r^+} \frac{\partial V_x^+}{\partial \varphi_+} - \frac{V_\varphi^{+2}}{r^+} \frac{\partial r^+}{\partial x_+} = \frac{C_2^2}{C_4^2} Ue^+ \frac{\partial Ue^+}{\partial x_+} + C_2 C_1^2 \frac{\partial^2 V_x^+}{\partial y_+^2} \quad (2)$$

$$V_x^+ \frac{\partial V_\varphi^+}{\partial x_+} + \frac{C_1 C_2}{C_3} V_y^+ \frac{\partial V_\varphi^+}{\partial y_+} + \frac{V_\varphi^+}{r^+} \frac{\partial V_\varphi^+}{\partial \varphi_+} + \frac{V_\varphi^+ V_x^+}{r^+} \frac{\partial r^+}{\partial x_+} = \frac{C_2^2}{C_4^2} \frac{Ue^+}{r^+} \frac{\partial Ue^+}{\partial \varphi_+} + C_2 C_1^2 \frac{\partial^2 V_\varphi^+}{\partial y_+^2} \quad (3)$$

With:

$Ue = \sqrt{Ue_x^2 + Ue_\varphi^2}$  : Modulus of external speed [7]

$Ue_x = U_\infty (A_\varphi \sin \alpha \sin \varphi)$  (4)

$Ue_\varphi = U_\infty (A_x \cos \alpha + B_x \sin \alpha \cos \varphi)$  (5)

$$A_x(x) = 0,68 + 3,0329x - 25,44074x^2 + 121,069x^3 + 318,64541x^4 + 466,99471x^5 - 356,01959x^6 + 110,24752x^7$$

$$B_x(x) = -0,80834 + 2,69424x - 21,37757x^2 + 98,83137x^3 - 252,98221x^4 + 363,05621x^5 - 272,50282x^6 + 83,5337x^7$$

$$A_\varphi = 2,3181 - 2,29665x + 5,87104x^2 - 10,90766x^3 + 10,3346x^4 - 4,06092x^5$$

• **Heatequation**

$$V_x^+ \frac{\partial T^+}{\partial x_+} + \frac{C_1 C_2}{C_3} V_y^+ \frac{\partial T^+}{\partial y_+} + \frac{V_\varphi^+}{r^+} \frac{\partial T^+}{\partial \varphi_+} = C_2 C_1^2 \frac{1}{Pr} \frac{\partial^2 T^+}{\partial y_+^2} \quad (6)$$

With  $Pr = \frac{\mu c_p}{\lambda} = \frac{\nu}{a}$  : Prandtl number

**2.3. Boundary conditions:**

On the wall:  $y=0$

$$T^+ = +1 \quad V_x^+(x_+, 0, \varphi_+) = 0$$

$$V_y^+(x_+, 0, \varphi_+) = 0 \quad V_\varphi^+(x_+, 0, \varphi_+) = r^+ C_2 \quad (7)$$

Away from the wall:  $y \rightarrow \infty$

$$T^+(x_+, y_+, \varphi_+) \rightarrow 0$$

$$V_x^+(x_+, y_+, \varphi_+) \rightarrow \frac{C_2}{C_4} Ue_x^+ V_\varphi^+(x_+, y_+, \varphi_+) \rightarrow \frac{C_2}{C_4} Ue_\varphi^+ \quad (8)$$

**2.4. Nusselt number and friction coefficients**

**a. Nusselt number**

$$2 C_5 C_1^{-1} Ec^{-1} Re_\infty^{-\frac{1}{2}} Nu = - \left( \frac{\partial T^+}{\partial y^+} \right)_{y_+=0} \quad (9)$$

With:

$Re_\infty = \frac{U_\infty L}{\nu}$ : Reynolds number

$Ec = \frac{U_\infty^2}{c_p \Delta T}$ : Eker number

**b. Friction coefficients**

$$\frac{1}{2} C_2 C_1^{-1} Re_\infty^{-\frac{1}{2}} C f u = \left( \frac{\partial V_x^+}{\partial y^+} \right)_{y_+=0} ; \frac{1}{2} C_2 C_1^{-1} Re_\infty^{-\frac{1}{2}} C f w = \left( \frac{\partial V_\varphi^+}{\partial y^+} \right)_{y_+=0} \quad (10)$$

**III. NUMERICAL SOLUTION**

The flow studied is three-dimensional and stationary around the cone. We take as mesh of the network of finite number  $L \times M \times N$  stacks of elementary curvilinear parallelepipeds attached to the body and defined by the steps  $\Delta x_+$ ,  $\Delta y_+$ ,  $\Delta \varphi_+$  where  $\Delta x_+$  is the dimensionless step of the curvilinear abscissa,  $\Delta y_+$  the dimensionless step of the normal coordinate and  $\Delta \varphi_+$  the dimensionless step of the azimuthal coordinate.  $L$ ,  $M$  and  $N$  are respectively the maximum registration indices along the curvilinear abscissa  $x$ , the normal coordinate  $y$  and the azimuthal coordinate  $\varphi$ .  $L$  and  $N$  directly related to the geometrical discretization of the body. As for  $M$ , it characterizes the thickness of the boundary layer which is not known a priori and which changes from one stack to another.

The value of the physical quantity  $G = G(x_+, y_+, \varphi_+)$  at the point  $(i, j, k)$  is noted  $G_{i,j}^k$

As for the dimensionless normal component is calculated from the continuity equation:

$$V_{i+1,j+1}^k = \frac{4V_{i+1,j}^k}{3} - \frac{V_{i+1,j-1}^k}{3} - \frac{2}{3} \Delta y_+ \left[ \frac{U_{i+1,j}^k U_{i,j}^k}{\Delta x_+} + \frac{W_{i+1,j}^{k+1} - W_{i+1,j}^{k-1}}{r_{i+1}^+ (2\Delta \varphi_+)} + \frac{U_{i+1,j}^k}{\Delta x_+} \left( \frac{r_{i+1}^+ - r_i^+}{r_{i+1}^+} \right) \right] \quad (11)$$

The values of  $V_{i+1,j+1}^k$  are calculated step by step by increasing values of  $j$  from the wall characterized by  $j = 1$ .

**Solving algorithm**

Each of these systems of equations associated with the boundary conditions and given by the equations, taken individually, can be written in the form:

$$A_j G_{j-1} + B_j G_j + C_j G_{j+1} = D_j, \quad 2 \leq j \leq J_{\max} \quad (12)$$

We proceed like Raminosa [8] and Alidina [9] who proposed by evaluating  $V_x^+$ ,  $V_y^+$ ,  $V_\varphi^+$  respectively at nodes  $[V_x^+]_{i+1}^k$ ,  $[V_y^+]_{i+1}^k$  and  $[V_\varphi^+]_{i+1}^k$ . This technique allows more reliable results to be obtained despite the sometimes very long execution time caused by the iterations that are required.

To lighten the notations, we pose:

$$U = V_x^+ ; V = V_y^+ ; W = V_\varphi^+ ; Ve = Ue^+ ; T = T^+ \quad (13)$$

$$\text{The convergence criterion is } \left| \frac{G_{i+1,j}^{k(n)} - G_{i+1,j}^{k(n-1)}}{\max(G_{i+1,j}^{k(n)}, G_{i+1,j}^{k(n+1)})} \right| \leq \varepsilon, \quad G = T, U, W \quad (14)$$

**IV. RESULTS AND DISCUSSION**

In this paper, we study the axisymmetric case and we fix  $Pr = 0.7$ ,  $\Delta x = 0.071428$ ,  $\Delta y = 0.0001$ ,  $L = 1m$ ,  $Re_\infty = 3000$  et  $\theta_0 = 20^\circ$ ,  $\alpha = 0^\circ$ .

$I_p = 2, 5, 7, 9, 11, 12$  and  $13$ , corresponds respectively to  $x_+ = 0.0714, 0.2857, 0.4286, 0.5714, 0.7143, 0.7857$  and  $0.8571$ .

Figures 2 and 3, illustrating the variations of the dimensionless temperature  $T^+$  as a function of  $y_+$ . On the one hand, at the wall, its value is maximum and is a decreasing function of  $y_+$  and on the other hand, it decreases as it moves away from the wall. In addition, if the coefficient  $B$  is large or the speed of the cone increases and far from the apex  $O$ , the radius of the cone is greater, then the variation in temperature is lower and this as  $y_+$  increases because of the speed of rotation of the cone and of fluid in forced convection, the heat could not be suitably transmitted by convection of particles which surround them and so on. This phenomenon is more marked for more distant particles. Moreover, we notice that the further we move away from the vertex  $O$ , the value of  $B$  seems more important.

Figure 4 illustrates the temperature variation curves as a function of  $x_+$  for  $\varphi = 60^\circ$  for several values of  $B$ . It is observed that, for  $y_+$  fixed, the temperature field is practically uniform on the wall except at the top. The curves in figures 5 and 6 show the meridian component of the velocity varies linearly in the boundary layer along the normal to the wall and that the thickness of the boundary layer changes very rapidly along the wall. However, close to the wall the effect of the speed of rotation of the cone and fluid in forced convection disrupts the flow. We also notice that far from the wall, the speed of rotation of the cone has no effect, only the speed of the fluid present there. Close to the wall, the further away from the top of the cone, the radius increases, the coefficient of rotation  $B$  becomes important, in other words, the speed of rotation increases, and that consequently the meridian component is less important because of the speed of the fluid. Figure 7 shows us the meridian component is uniform over the circumference of the cone.

Figures 8 and 9 illustrating the variations of the dimensionless normal component  $V_y^+$  as a function of  $y_+$ , show us that the fluid is sucked in by the wall.

Figure 10 illustrates the variations of the local Nusselt number against  $x^+$ , for several values of  $B$ . The results show that the heat exchange between the wall and the fluid takes place in a practically uniform manner along the surface of the cone, with the exception of the leading edge where the disturbance of the flow causes the exchange to decrease slightly of heat on the less exposed side. We give in Figure 11 the variations of the meridian parietal friction coefficient against  $x^+$ , for several values of  $B$ . It shows the wall tension is maximum near the ends of the cone, the site of strong flow disturbance.

## V. CONCLUSION

We carried out a numerical study of the flow and heat transfer in the boundary layer developed around a cone rotating around its axis of revolution and plunged into an ascending vertical forced flow. The transfer equations were solved by an implicit finite difference scheme. The results show in particular that the rapid variation in the rotational speed of the body generates a strong disturbance of the flow in the vicinity of the contact circumference and that the evolution of the external speed field is complex. This evolution is justified by the wall friction coefficient along the meridian line. The influence analysis of the rotational speed is represented by the rotation parameter  $B$  and the study is carried out within the framework of axisymmetric flow ( $\alpha = 0$ ). The perspective and the limit of this work are based on mixed convection: rotary, forced, natural and the variation of the angle of inclination and as well as the opening at the top of this cone.

## ACKNOWLEDGEMENTS

Authors would like to thank the science faculty and higher normal school ENSET of the Antsiranana University for the realization of this study. Authors wish also to thank the contribution of Journal AJER for the publication this paper.

## REFERENCES

- [1] F. A. RAKOTOMANGA and E. ALIDINA, Transfert thermiques convectifs tridimensionnels autour d'un cône de révolution, *Congres Français de Thermique*, 2013, Gérardmer, France.
- [2] G. BEZANDRY, R. RANDRIANARIVELO, U. CANISSIUS and E. ALIDINA, Etude numérique de la convection rotatoire pure autour d'un cône de révolution, *Rev. Ivoir. Sci. Technol*, 29, (2017)1 – 15.
- [3] U. CANISSIUS, F. A. RAKOTOMANGA and E. ALIDINA, Etude numérique de la convection naturelle tridimensionnelle d'un cône de révolution incliné, *Afrique SCIENCE*, 11(1), (2015) 1 – 11.
- [4] M. ABDALLAH and B. ZEGHMATI, Natural Convection Heat and Mass Transfer in the Boundary Layer along a Vertical Cylinder with Opposing Buoyancies, *Journal of Applied Fluid Mechanics*, 4(4), (2011)15 – 21.
- [5] Ch. R. R. RAMINOSOA, M. DAGUENET, Convection mixte autour d'une sphère. Influence de la variabilité des propriétés physiques du fluide, *Revue Générale de Thermique*, 1994.
- [6] A. ALI CHERIF, Ch. R. R. RAMINOSOA, M. RAKOTOMALALA, A. DAÏF et M. DAGUENET, Contrôle hydrodynamique des couches limites thermiques en convection mixte autour d'ellipsoïdes aplatis asymétriques, *Elsevier Science Ltd.*, 1996.
- [7] FRANCOIS D'ASSISE RAKOTOMANGA, Contribution à l'étude des transferts thermiques convectifs tridimensionnels autour d'un cône de révolution. *Doctoral Thesis*, Antsiranana University, Madagascar, (2013) 134p.
- [8] Ch. R. R. RAMINOSOA, Convection mixte a propriétés physiques variables autour d'un corps a symétrie de révolution, *Doctoral Thesis*, Antananarivo University, Madagascar, 1995.
- [9] E ALIDINA, Contribution à l'étude d'une convection mixte tridimensionnelle autour d'un ellipsoïde de révolution dans un écoulement ascendant de fluide newtonien, *State Doctoral thesis*, Antananarivo University, Madagascar, 1997.
- [10] M. S. RAKOTOMALALA, Etude des transferts dans la couche limite entourant un corps a symétrie de révolution tournant dans un fluide en présence d'un écoulement axial et d'une convection naturelle, *State Doctoral thesis*, Nice-Sophia Antipolis University, France, 1994.

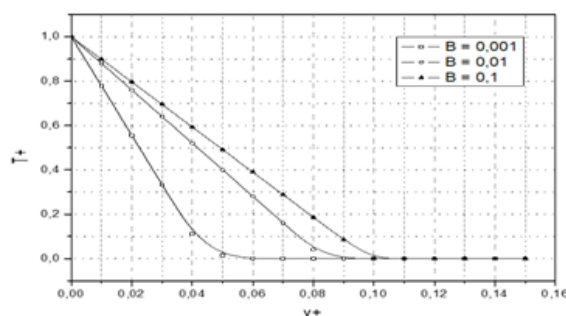


**Figure 2:** Dimensionless temperature evolution against  $y_+$  for  $\theta_0 = 20^\circ$ ,  $\phi = 60^\circ$  and several

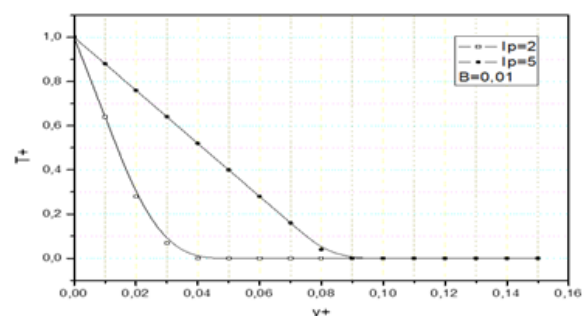


**Figure 3:** Dimensionless temperature evolution against  $y_+$  for  $\theta_0 = 20^\circ$ ,  $\phi = 60^\circ$ ,  $B = 0.1$  and several

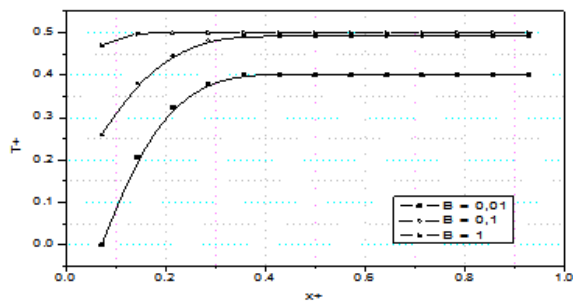


Figure 4: Dimensionless temperature evolution against  $x_+$  for several values of  $B$

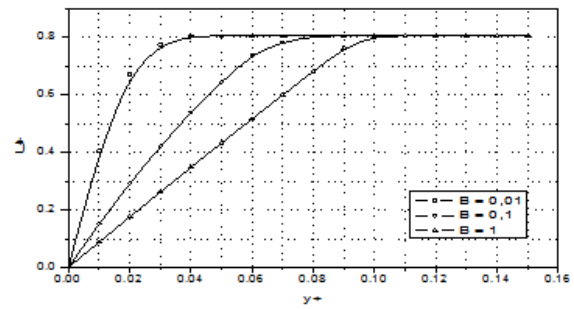


Figure 5: Dimensionless meridional velocity evolution against  $y_+$  for several values of  $B$

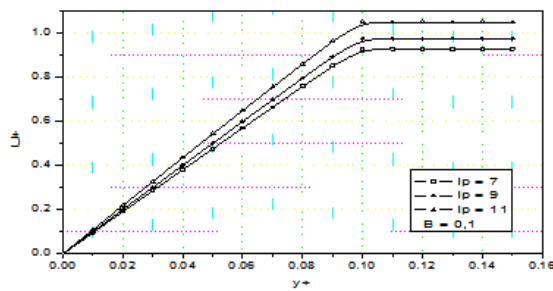


Figure 6: Dimensionless meridional velocity evolution against  $y_+$  for several values of  $I_p$  and  $B = 0.1$ .

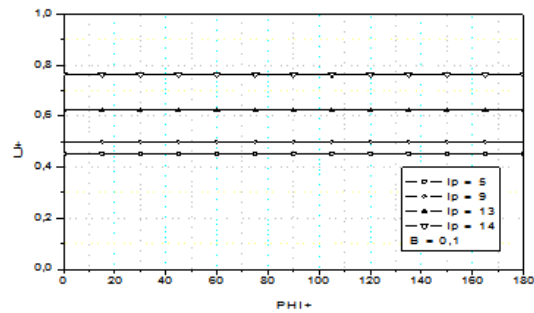


Figure 7: Dimensionless meridional velocity evolution against  $\phi$  for several values of  $I_p$  and  $B = 0.1$

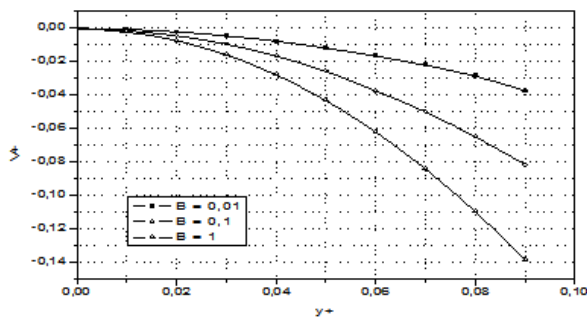


Figure 8: Dimensionless normal velocity evolution against  $y_+$  for several values of  $B$

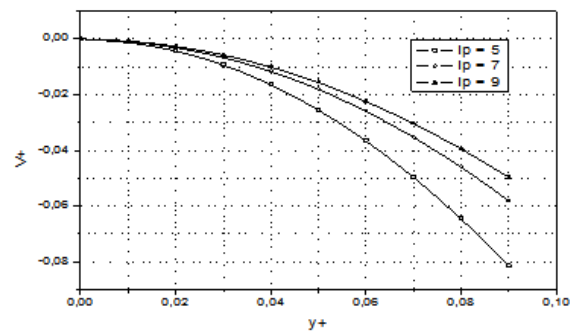


Figure 9: Dimensionless normal velocity evolution against  $y_+$  for several values of  $I_p$ .

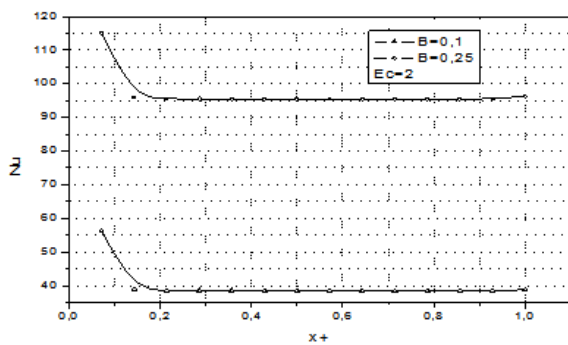


Figure 10: Nusselt number against  $x_+$  for several values of  $B$

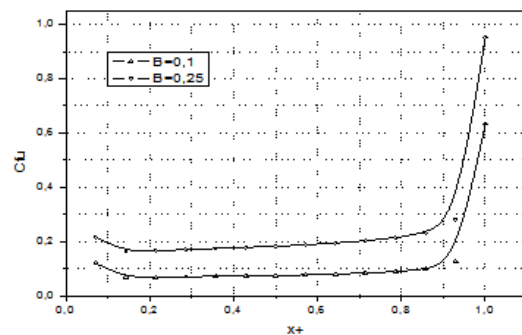


Figure 11: Meridianparietal friction coefficient against  $x_+$  for several values of  $B$